Structural Engineering and Mechanics, Vol. 29, No. 5 (2008) 531-550
DOI: http://dx.doi.org/10.12989/sem.2008.29.5.531

On the natural frequencies and mode shapes of a multi-span and multi-step beam carrying a number of concentrated elements

Hsien-Yuan Lin†

Department of Mechanical Engineering, Cheng Shiu University, Kaohsiung 833, Taiwan, Republic of China

(Received September 6, 2007, Accepted May 23, 2008)

Abstract. This paper adopts the numerical assembly method (NAM) to determine the exact solutions of natural frequencies and mode shapes of a multi-span and multi-step beam carrying a number of various concentrated elements including point masses, rotary inertias, linear springs, rotational springs and spring-mass systems. First, the coefficient matrix for an intermediate station with various concentrated elements, cross-section change and/or pinned support and the ones for the left-end and right-end supports of a beam are derived. Next, the overall coefficient matrix for the entire beam is obtained using the numerical assembly technique of the conventional finite element method (FEM). Finally, the exact solutions for the natural frequencies of the vibrating system are determined by equating the determinant of the last overall coefficient matrix to zero and the associated mode shapes are obtained by substituting the corresponding values of integration constants into the associated eigenfunctions.

Keywords: multi-step beam; exact solution; natural frequency; mode shape.

1. Introduction

For a single-step beam, Balasubramanian *et al.* (1985,1990) and Subramanian (1985) investigated their free vibration characteristics. Jang and Bert (1989a, 1989b) reported its exact and approximate solutions for the natural frequencies under various boundary conditions. Maurizi and Belles (1994) studied the natural frequencies of the one-span beams with stepwise variable cross-sections. Lee and Bergman (1994) used the elemental dynamic flexibility method to study the free and forced vibrations of the seven-step beam. Ju *et al.* (1994) used a first order shear deformation theory and the corresponding finite element formulation to analyze the free vibration of the two-step beams. De Rosa (1994) and De Rosa *et al.* (1995) deduced the free vibration frequencies of a single-step beam by solving the differential equations of motion and the associated eigenvalue problem. Naguleswaran (2002a) found the natural frequencies and mode shapes of an Euler-Bernoulli beam on classical end supports and with one-step change in cross-section by equating the second order determinant to zero, and also the natural frequencies of an Euler-Bernoulli beam on elastic end supports and with up to three-step changes in cross-sections by equating the fourth order

† Associate Professor, Ph.D., E-mail: lin.syg@msa.hinet.net, linsyg@csu.edu.tw

determinant to zero (2002b).

For the uniform beams, Hamdan and Abdel (1994) found the exact natural frequencies of a uniform beam with attached inertia elements. Wu and Chou (1998) found the approximate natural frequencies and mode shapes of a uniform beam carrying any number of elastically attached lumped masses by means of the analytical-and -numerical-combined method (ANCM). Later, Wu and Chou (1999) obtained the exact solution of the similar vibrating system by using the numerical assembly method (NAM). By means of the same method (NAM), Chen and Wu (2002) and Chen (2003) obtained the exact solutions for the natural frequencies and mode shapes of the non-uniform (wedge) beams carrying multiple spring-mass systems or other various concentrated elements including point masses, linear springs and rotational springs. Lin and Tsai (2005,2007)determined the exact values of natural frequencies and associated mode shapes of a "multi-span" uniform beam carrying a number of point masses, spring-mass systems and "multi-step" beam carrying a number of point masses and rotary inertias (2006) with the NAM. The objective of this paper is to extend the theory of NAM to investigate the free vibration characteristics of a multi-span and multi-step beam carrying various concentrated elements including point masses, rotary inertias, linear springs, rotational springs and spring-mass systems. For convenience, a beam without any attachments is called "bare" beam and a beam carrying any attachments is called "loaded" beam, in this paper.

2. Equation of motion and displacement function

Fig. 1 shows the sketch of a pinned-pinned beam with V-step changes in cross-sections and carrying various concentrated elements. The points corresponding to the locations of the V-step changes in cross-sections, simple supports, lumped masses, rotary inertias, linear springs, rotational springs and/or spring-mass systems are referred to as "stations".

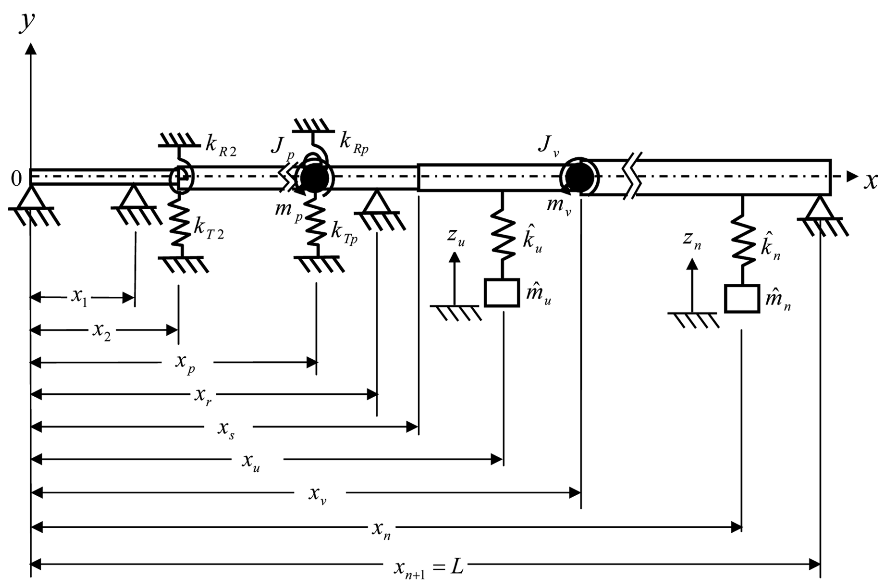

Fig. 1 Sketch for a pinned-pinned beam with multiple intermediate rigid (pinned) supports, multiple step changes in cross-sections and carrying various concentrated elements

The differential equation of motion for the i-th beam segment is given by

$$EI_i\frac{\partial^4 y_i(x,t)}{\partial x^4}+\overline{m}_i\frac{\partial^2 y_i(x,t)}{\partial^2 t} = 0 \qquad i = 1,2,\ldots,\overline{n} \tag{1}$$

where E is Young's modulus, I_i is moment of inertia of cross-sectional area of the i-th beam segment, $\overline{m}_i$ is mass per unit length of the i-th beam segment, $y_i(x,t)$ is transverse displacement at position x and time t for the i-th beam segment.

For free vibrations, one has

$$y_i(x,t) = Y_i(x)e^{j\omega t} \tag{2}$$

where $Y_i(x)$ is the amplitude of $y_i(x,t)$, ω is the natural frequency of the beam and $j = \sqrt{-1}$.

Substitution of Eq. (2) into Eq. (1) gives

$$Y_i''''(x)-\beta_{v,i}^4 Y_i(x) = 0 \tag{3}$$

where $\beta_{v,i}$ is the frequency parameter for the i-th beam segment corresponding to the v-th vibration mode defined by

$$\beta_{v,i}^4 = \frac{\omega_v^2\overline{m}_i}{EI_i} \tag{4a}$$

or

$$\omega_v = (\beta_{v,i}L)^2\left(\frac{EI}{\overline{m}_i L^4}\right)^{1/2} = \Omega_{v,i}^2\left(\frac{EI_i}{\overline{m}_i L^4}\right)^{1/2} \tag{4b}$$

with

$$\Omega_{v,i} = \beta_{v,i}L \tag{4c}$$

where $\Omega_{v,i}$ is dimensionless frequency parameter for the i-th beam segment corresponding to the v-th vibration mode.

The general solution of Eq. (3) takes the form

$$Y_i(x) = C_{i,1}\sin(\beta_{v,i}x)+C_{i,2}\cos(\beta_{v,i}x)+C_{i,3}\sinh(\beta_{v,i}x)+C_{i,4}\cosh(\beta_{v,i}x) \tag{5}$$

which is the displacement function for the i-th beam segment located at the left side of the i-th station.

3. Coefficient matrices for intermediate stations and ends of the beam

At the arbitrary station i located at $x = x_i$ (see Fig. 1), from Eq. (5) one has

$$Y_i(\xi_i) = C_{i,1}\sin(\Omega_{v,i}\xi_i)+C_{i,2}\cos(\Omega_{v,i}\xi_i)+C_{i,3}\sinh(\Omega_{v,i}\xi_i)+C_{i,4}\cosh(\Omega_{v,i}\xi_i) \tag{6}$$

$$Y_i'(\xi_i) = \Omega_{v,i}[C_{i,1}\cos(\Omega_{v,i}\xi_i)-C_{i,2}\sin(\Omega_{v,i}\xi_i)+C_{i,3}\cosh(\Omega_{v,i}\xi_i)+C_{i,4}\sinh(\Omega_{v,i}\xi_i)] \tag{7}$$

$$Y_i''(\xi_i) = \Omega_{v,i}^2[-C_{i,1}\sin(\Omega_{v,i}\xi_i) - C_{i,2}\cos(\Omega_{v,i}\xi_i) + C_{i,3}\sinh(\Omega_{v,i}\xi_i) + C_{i,4}\cosh(\Omega_{v,i}\xi_i)] \tag{8}$$

$$Y_i'''(\xi_i) = \Omega_{v,i}^3[-C_{i,1}\cos(\Omega_{v,i}\xi_i) + C_{i,2}\sin(\Omega_{v,i}\xi_i) + C_{i,3}\cosh(\Omega_{v,i}\xi_i) + C_{i,4}\sinh(\Omega_{v,i}\xi_i)] \tag{9}$$

with

$$\xi_i = x_i/L \tag{10}$$

In Eqs. (7), (8) and (9), the primes refer to differentiations with the respect to the coordinate x_i.

3.1 Coefficient matrix [B_p] for an intermediate cross-section or/and concentrated element

If the station numbering of an intermediate step change in cross-section, point mass, rotary inertia, linear spring and rotational spring is p, then the continuity of deformations and the equilibrium of moments and forces at station p require that

$$Y_p(\xi_p) = Y_{p+1}(\xi_p) \tag{11a}$$

$$Y_p'(\xi_p) = Y_{p+1}'(\xi_p) \tag{11b}$$

$$Y_p''(\xi_p) - \left[J_p^*\Omega_{v,p}^4\left(\frac{\overline{m}_1}{\overline{m}_p}\right) - k_{Rp}^*\left(\frac{I_1}{I_p}\right)\right]Y_p'(\xi_p) = \varepsilon_p Y_{p+1}''(\xi_p) \tag{11c}$$

$$Y_p'''(\xi_p) + \left[m_p^*\Omega_{v,p}^4\left(\frac{\overline{m}_1}{\overline{m}_p}\right) - k_{Tp}^*\left(\frac{I_1}{I_p}\right)\right]Y_p(\xi_p) = \varepsilon_p Y_{p+1}'''(\xi_p) \tag{11d}$$

$$m_p^* = \frac{m_p}{\overline{m}_1 L},\quad J_p^* = \frac{J_p}{\overline{m}_1 L^3},\quad k_{Rp}^* = \frac{k_{Rp}L}{EI_1},\quad k_{Tp}^* = \frac{k_{Tp}L^3}{EI_1},\quad \varepsilon_p = \frac{I_{p+1}}{I_p} \tag{12a,b,c,d,e}$$

where m_p, J_p, k_{Rp} and k_{Tp} are respectively the lumped mass , rotary inertia, rotational spring constant and linear spring constant at the p-th station.

Substitution of Eqs. (6)-(9) into Eqs. (11a)-(11d) leads to

$$C_{p,1}\sin(\Omega_{v,p}\xi_p) + C_{p,2}\cos(\Omega_{v,p}\xi_p) + C_{p,3}\sinh(\Omega_{v,p}\xi_p) + C_{p,4}\cosh(\Omega_{v,p}\xi_p)$$
$$- C_{p+1,1}\sin(\Omega_{v,p+1}\xi_p) - C_{p+1,2}\cos(\Omega_{v,p+1}\xi_p) - C_{p+1,3}\sinh(\Omega_{v,p+1}\xi_p) - C_{p+1,4}\cosh(\Omega_{v,p+1}\xi_p) = 0 \tag{13a}$$

$$\Omega_{v,p}[C_{p,1}\cos(\Omega_{v,p}\xi_p) - C_{p,2}\sin(\Omega_{v,p}\xi_p) + C_{p,3}\cosh(\Omega_{v,p}\xi_p) + C_{p,4}\sinh(\Omega_{v,p}\xi_p)]$$
$$-\Omega_{v,p+1}[C_{p+1,1}\cos(\Omega_{v,p+1}\xi_p) - C_{p+1,2}\sin(\Omega_{v,p+1}\xi_p) + C_{p+1,3}\cosh(\Omega_{v,p+1}\xi_p) + C_{p+1,4}\sinh(\Omega_{v,p+1}\xi_p)] = 0 \tag{13b}$$

$$\Omega_{v,p}^2[-C_{p,1}\sin(\Omega_{v,p}\xi_p) - C_{p,2}\cos(\Omega_{v,p}\xi_p) + C_{p,3}\sinh(\Omega_{v,p}\xi_p) + C_{p,4}\cosh(\Omega_{v,p}\xi_p)]$$
$$-\left[J_p^*\Omega_{v,p}^4\left(\frac{\overline{m}_1}{\overline{m}_p}\right) - k_{Rp}^*\left(\frac{I_1}{I_p}\right)\right]\Omega_{v,p}[C_{p,1}\cos(\Omega_{v,p}\xi_p) - C_{p,2}\sin(\Omega_{v,p}\xi_p) + C_{p,3}\cosh(\Omega_{v,p}\xi_p) + C_{p,4}\sinh(\Omega_{v,p}\xi_p)]$$
$$-\varepsilon_p\Omega_{v,p+1}^2[-C_{p+1,1}\sin(\Omega_{v,p+1}\xi_p) - C_{p+1,2}\cos(\Omega_{v,p+1}\xi_p) + C_{p+1,3}\sinh(\Omega_{v,p+1}\xi_p) + C_{p+1,4}\cosh(\Omega_{v,p+1}\xi_p)] = 0 \tag{13c}$$

$$\Omega_{v,p}^{3}[-C_{p,1}\cos(\Omega_{v,p}\xi_p)+C_{p,2}\sin(\Omega_{v,p}\xi_p)+C_{p,3}\cosh(\Omega_{v,p}\xi_p)+C_{p,4}\sinh(\Omega_{v,p}\xi_p)]$$
$$+\left[m_p^*\Omega_{v,p}^4\left(\frac{\overline{m}_1}{\overline{m}_p}\right)-k_{Tp}^*\left(\frac{I_1}{I_p}\right)\right][C_{p,1}\sin(\Omega_{v,p}\xi_p)+C_{p,2}\cos(\Omega_{v,p}\xi_p)+C_{p,3}\sinh(\Omega_{v,p}\xi_p)+C_{p,4}\cosh(\Omega_{v,p}\xi_p)]$$
$$-\varepsilon_p\Omega_{v,p+1}^{3}[-C_{p+1,1}\cos(\Omega_{v,p+1}\xi_p)+C_{p+1,2}\sin(\Omega_{v,p+1}\xi_p)+C_{p+1,3}\cosh(\Omega_{v,p+1}\xi_p)+C_{p+1,4}\sinh(\Omega_{v,p+1}\xi_p)]=0 \tag{13d}$$

Writing Eqs. (13a)-(13d) in matrix form, one has

$$[B_p]\{C_p\} = 0 \tag{14}$$

where

$$\{C_p\} = \{C_{p,1}\ \ C_{p,2}\ \ C_{p,3}\ \ C_{p,4}\ \ C_{p+1,1}\ \ C_{p+1,2}\ \ C_{p+1,3}\ \ C_{p+1,4}\} \tag{15}$$

In the above Eqs. (14) and (15), the symbols, [ ] and { }, denote the rectangular matrix and column vector, respectively. The coefficient matrix $[B_p]$ is placed in Appendix A at the end of this paper.

3.2 Coefficient matrix [B_u] for an intermediate spring-mass system

If the station numbering of an intermediate spring-mass system is u, then the continuity of deformations and the equilibrium of moments and forces at station u require that

$$Y_u(\xi_u) = Y_{u+1}(\xi_u) \tag{16a}$$

$$Y_u'(\xi_u) = Y_{u+1}'(\xi_u) \tag{16b}$$

$$Y_u''(\xi_u) = \varepsilon_u Y_{u+1}''(\xi_u) \tag{16c}$$

$$Y_u'''(\xi_u) + \hat{m}_u^*\Omega_{v,u}^4\left(\frac{\overline{m}_1}{\overline{m}_u}\right)Z_u = \varepsilon_u Y_{u+1}'''(\xi_u) \tag{16d}$$

$$\hat{m}_u^* = \hat{m}_u/(\overline{m}_1 L) \tag{17}$$

where $\hat{m}_u$ is the mass of intermediate spring-mass system and Z_u is the displacement amplitude of $\hat{m}_u$ at the u-th station.

Substitution of Eqs. (6)-(9) into Eqs. (16a)-(16d) leads to

$$C_{u,1}\sin(\Omega_{v,u}\xi_u)+C_{u,2}\cos(\Omega_{v,u}\xi_u)+C_{u,3}\sinh(\Omega_{v,u}\xi_u)+C_{u,4}\cosh(\Omega_{v,u}\xi_u)$$
$$-C_{u+1,1}\sin(\Omega_{v,u+1}\xi_u)-C_{u+1,2}\cos(\Omega_{v,u+1}\xi_u)-C_{u+1,3}\sinh(\Omega_{v,u+1}\xi_u)-C_{u+1,4}\cosh(\Omega_{v,u+1}\xi_u) = 0 \tag{18a}$$

$$\Omega_{v,u}[C_{u,1}\cos(\Omega_{v,u}\xi_u)-C_{u,2}\sin(\Omega_{v,u}\xi_u)+C_{u,3}\cosh(\Omega_{v,u}\xi_u)+C_{u,4}\sinh(\Omega_{v,u}\xi_u)]$$
$$-\Omega_{v,u+1}[C_{u+1,1}\cos(\Omega_{v,u+1}\xi_u)-C_{u+1,2}\sin(\Omega_{v,u+1}\xi_u)+C_{u+1,3}\cosh(\Omega_{v,u+1}\xi_u)+C_{u+1,4}\sinh(\Omega_{v,u+1}\xi_u)]=0 \tag{18b}$$

$$\Omega_{v,u}^2[-C_{u,1}\sin(\Omega_{v,u}\xi_u)-C_{u,2}\cos(\Omega_{v,u}\xi_u)+C_{u,3}\sinh(\Omega_{v,u}\xi_u)+C_{u,4}\cosh(\Omega_{v,u}\xi_u)]$$
$$-\varepsilon_u\Omega_{v,u+1}^2[-C_{u+1,1}\sin(\Omega_{v,u+1}\xi_u)-C_{u+1,2}\cos(\Omega_{v,u+1}\xi_u)+C_{u+1,3}\sinh(\Omega_{v,u+1}\xi_u)+C_{u+1,4}\cosh(\Omega_{v,u+1}\xi_u)]=0 \tag{18c}$$

$$\Omega_{v,u}^3[-C_{u,1}\cos(\Omega_{v,u}\xi_u)+C_{u,2}\sin(\Omega_{v,u}\xi_u)+C_{u,3}\cosh(\Omega_{v,u}\xi_u)+C_{u,4}\sinh(\Omega_{v,u}\xi_u)]+\hat{m}_u^*\Omega_{v,u}^4\left(\frac{\overline{m}_1}{\overline{m}_u}\right)Z_u$$
$$-\varepsilon_u\Omega_{v,u+1}^3[-C_{u+1,1}\cos(\Omega_{v,u+1}\xi_u)+C_{u+1,2}\sin(\Omega_{v,u+1}\xi_u)+C_{u+1,3}\cosh(\Omega_{v,u+1}\xi_u)+C_{u+1,4}\sinh(\Omega_{v,u+1}\xi_u)]$$
$$=0 \tag{18d}$$

For the spring-mass system at station u, its equation of motion is given by

$$\hat{m}_u\ddot{z}_u+\hat{k}_u(z_u-y_u)=0 \tag{19}$$

where $\hat{k}_u$ is the spring constant of intermediate spring-mass system and z_u is the displacement of $\hat{m}_u$ relative to the static beam at the u-th station, as one may see from Fig. 1.

When the spring-mass system performs free vibrations, one has

$$z_u(t)=Z_ue^{j\omega t} \tag{20}$$

The substitution of Eqs. (2) and (20) into Eq. (19) gives

$$\hat{k}_uY_u-(\hat{k}_u-\hat{m}_u\omega^2)Z_u=0 \tag{21}$$

or

$$Y_u+(\lambda_u^2-1)Z_u=0 \tag{22}$$

where

$$\lambda_u=\omega/\hat{\omega}_u \tag{23}$$

with

$$\hat{\omega}_u=\sqrt{\hat{k}_u/\hat{m}_u} \tag{24}$$

The substitution of Eq. (6) into Eq. (22) leads to

$$C_{u,1}\sin(\Omega_{v,u}\xi_u)+C_{u,2}\cos(\Omega_{v,u}\xi_u)+C_{u,3}\sinh(\Omega_{v,u}\xi_u)+C_{u,4}\cosh(\Omega_{v,u}\xi_u)+(\lambda_u^2-1)Z_u=0 \tag{18e}$$

Writing Eqs. (18a)-(18e) in matrix form, one has

$$[B_u]\{C_u\}=0 \tag{25}$$

where

$$\{C_u\}=\{C_{u,1}\ \ C_{u,2}\ \ C_{u,3}\ \ C_{u,4}\ \ C_{u+1,1}\ \ C_{u+1,2}\ \ C_{u+1,3}\ \ C_{u+1,4}\ \ Z_u\} \tag{26}$$

and the coefficient matrix $[B_u]$ is placed in Appendix B at the end of this paper.

3.3 Coefficient matrix $[B_r]$ for an intermediate rigid support

Similarly, if the station numbering of an intermediate rigid support is r, then the continuity of deformations and the equilibrium of moments at station r require that

$$Y_r(\xi_r) = Y_{r+1}(\xi_r) = 0 \tag{27a,b}$$

$$Y_r'(\xi_r) = Y_{r+1}'(\xi_r) \tag{27c}$$

$$Y_r''(\xi_r) = \varepsilon_r Y_{r+1}''(\xi_r) \tag{27d}$$

Introducing Eqs. (6)-(9) into Eq. (27), one obtains

$$C_{r,1}\sin(\Omega_{v,r}\xi_r) + C_{r,2}\cos(\Omega_{v,r}\xi_r) + C_{r,3}\sinh(\Omega_{v,r}\xi_r) + C_{r,4}\cosh(\Omega_{v,r}\xi_r) = 0 \tag{28a}$$

$$C_{r+1,1}\sin(\Omega_{v,r+1}\xi_r) + C_{r+1,2}\cos(\Omega_{v,r+1}\xi_r) + C_{r+1,3}\sinh(\Omega_{v,r+1}\xi_r) + C_{r+1,4}\cosh(\Omega_{v,r+1}\xi_r) = 0 \tag{28b}$$

$$\begin{gathered}\Omega_{v,r}[C_{r,1}\cos(\Omega_{v,r}\xi_r) - C_{r,2}\sin(\Omega_{v,r}\xi_r) + C_{r,3}\cosh(\Omega_{v,r}\xi_r) + C_{r,4}\sinh(\Omega_{v,r}\xi_r)] \\ -\Omega_{v,r+1}[C_{r+1,1}\cos(\Omega_{v,r+1}\xi_r) - C_{r+1,2}\sin(\Omega_{v,r+1}\xi_r) + C_{r+1,3}\cosh(\Omega_{v,r+1}\xi_r) + C_{r+1,4}\sinh(\Omega_{v,r+1}\xi_r)] = 0\end{gathered} \tag{28c}$$

$$\begin{gathered}\Omega_{v,r}^2[-C_{r,1}\sin(\Omega_{v,r}\xi_r) - C_{r,2}\cos(\Omega_{v,r}\xi_r) + C_{r,3}\sinh(\Omega_{v,r}\xi_r) + C_{r,4}\cosh(\Omega_{v,r}\xi_r)] \\ -\varepsilon_r\Omega_{v,r+1}^2[-C_{r+1,1}\sin(\Omega_{v,r+1}\xi_r) - C_{r+1,2}\cos(\Omega_{v,r+1}\xi_r) + C_{r+1,3}\sinh(\Omega_{v,r+1}\xi_r) + C_{r+1,4}\cosh(\Omega_{v,r+1}\xi_r)] = 0\end{gathered} \tag{28d}$$

or

$$[B_r]\{C_r\} = 0 \tag{29}$$

where
$$\{C_r\} = \{C_{r,1}\ \ C_{r,2}\ \ C_{r,3}\ \ C_{r,4}\ \ C_{r+1,1}\ \ C_{r+1,2}\ \ C_{r+1,3}\ \ C_{r+1,4}\} \tag{30}$$

and the coefficient matrix $[B_r]$ is placed in Appendix C at the end of this paper.

3.4 Coefficient matrix $[B_0]$ for the left end of the entire beam

If the left-end support of the beam is pinned as shown in Fig. 1, then the boundary conditions are

$$Y_0(0) = Y_0''(0) = 0 \tag{31a, b}$$

The substitution of Eqs. (6) and (8) into Eqs. (31a) and (31b) leads to

$$C_{0,2} + C_{0,4} = 0 \tag{32a}$$

$$-C_{0,2} + C_{0,4} = 0 \tag{32b}$$

or in matrix form

$$[B_0]\{C_0\} = 0 \tag{33}$$

where

$$[B_0] = \begin{array}{c} \begin{matrix} 1 & 2 & 3 & 4 \end{matrix} \\ \begin{bmatrix} 0 & 1 & 0 & 1 \\ 0 & -1 & 0 & 1 \end{bmatrix} \end{array} \begin{matrix} \\ 1 \\ 2 \end{matrix} \tag{34}$$

$$\{C_0\} = \{C_{0,1} \;\; C_{0,2} \;\; C_{0,3} \;\; C_{0,4}\} \tag{35}$$

Similarly, if the left-end support of the beam is free, then the boundary conditions are

$$Y_0''(0) = Y_0'''(0) = 0 \tag{36a, b}$$

and the boundary coefficient matrix is given by

$$[B_0] = \begin{array}{c} \begin{matrix} 1 & 2 & 3 & 4 \end{matrix} \\ \begin{bmatrix} 0 & -1 & 0 & 1 \\ -1 & 0 & 1 & 0 \end{bmatrix} \end{array} \begin{matrix} \\ 1 \\ 2 \end{matrix} \tag{37}$$

If the left-end support of the beam is clamped, one obtains the following boundary coefficient matrix

$$[B_0] = \begin{array}{c} \begin{matrix} 1 & 2 & 3 & 4 \end{matrix} \\ \begin{bmatrix} 0 & 1 & 0 & 1 \\ 1 & 0 & 1 & 0 \end{bmatrix} \end{array} \begin{matrix} \\ 1 \\ 2 \end{matrix} \tag{38}$$

3.5 Coefficient matrix [B_{n+1}] for the right end of the entire beam

If the right-end support of the beam is pinned as shown in Fig. 1, then the boundary conditions are

$$Y_{n+1}(L) = Y''_{n+1}(L) = 0 \tag{39a, b}$$

Where n is the total number of intermediate stations.

Substituting Eqs. (6) and (8) into Eqs. (39a) and (39b), one obtains

$$C_{n+1,1}\sin\Omega_{v,n+1} + C_{n+1,2}\cos\Omega_{v,n+1} + C_{n+1,3}\sinh\Omega_{v,n+1} + C_{n+1,4}\cosh\Omega_{v,n+1} = 0 \tag{40a}$$

$$-C_{n+1,1}\sin\Omega_{v,n+1} - C_{n+1,2}\cos\Omega_{v,n+1} + C_{n+1,3}\sinh\Omega_{v,n+1} + C_{n+1,4}\cosh\Omega_{v,n+1} = 0 \tag{40b}$$

or

$$[B_{n+1}]\{C_{n+1}\} = 0 \tag{41}$$

where

$$[B_{n+1}] = \begin{array}{c} \begin{matrix} 4n+1 & 4n+2 & 4n+3 & 4n+4 \end{matrix} \\ \begin{bmatrix} \sin\Omega_{v,n+1} & \cos\Omega_{v,n+1} & \sinh\Omega_{v,n+1} & \cosh\Omega_{v,n+1} \\ -\sin\Omega_{v,n+1} & -\cos\Omega_{v,n+1} & \sinh\Omega_{v,n+1} & \cosh\Omega_{v,n+1} \end{bmatrix} \end{array} \begin{matrix} \\ q-1 \\ q \end{matrix} \tag{42}$$

$$\{C_{n+1}\} = \{C_{n+1,1} \;\; C_{n+1,2} \;\; C_{n+1,3} \;\; C_{n+1,4}\} \tag{43a}$$

In Eq. (42), q denotes the total number of equations for the integration constants given by

$$q = 4(n+1)+S \tag{43b}$$

where S denotes the total number of spring-mass systems attached to the beam.

Similarly, if the right-end support of the beam is clamped, then the boundary conditions are

$$Y_{n+1}(L) = Y'_{n+1}(L) = 0 \tag{44a, b}$$

and the boundary coefficient matrix is given by

$$[B_{n+1}] = \begin{array}{c} \begin{array}{cccc} 4n+1 & 4n+2 & 4n+3 & 4n+4 \end{array} \\ \begin{bmatrix} \sin\Omega_{v,n+1} & \cos\Omega_{v,n+1} & \sinh\Omega_{v,n+1} & \cosh\Omega_{v,n+1} \\ \cos\Omega_{v,n+1} & -\sin\Omega_{v,n+1} & \cosh\Omega_{v,n+1} & \sinh\Omega_{v,n+1} \end{bmatrix} \end{array} \begin{array}{c} \\ q-1 \\ q \end{array} \tag{45}$$

If the right-end support of the beam is free, one obtains the following boundary coefficient matrix

$$[B_{n+1}] = \begin{array}{c} \begin{array}{cccc} 4n+1 & 4n+2 & 4n+3 & 4n+4 \end{array} \\ \begin{bmatrix} -\sin\Omega_{v,n+1} & -\cos\Omega_{v,n+1} & \sinh\Omega_{v,n+1} & \cosh\Omega_{v,n+1} \\ -\cos\Omega_{v,n+1} & \sin\Omega_{v,n+1} & \cosh\Omega_{v,n+1} & \sinh\Omega_{v,n+1} \end{bmatrix} \end{array} \begin{array}{c} \\ q-1 \\ q \end{array} \tag{46}$$

4. Determination of natural frequencies and mode shapes of the beam

The integration constants relating to the left-end and right-end supports of the beam are defined by Eqs. (35) and (43), respectively, while those relating to the intermediate stations are defined by Eqs. (15), (26) and/or (30) depending upon step change in cross-section, point mass, rotary inertia, linear spring, rotational spring, spring-mass system and/or rigid (pinned) support being located there. The associated coefficient matrices are given by $[B_0]$ (cf. Eqs. (34), (37) or (38)), $[B_p]$ (cf. Eq. (A1) of Appendix A), $[B_u]$ (cf. Eq. (B1) of Appendix B), $[B_r]$ (cf. Eq. (C1) of Appendix C) and $[B_{n+1}]$ (cf. Eqs. (42), (45) or (46)). From the last equations concerned one may see that the identification number for each element of the last coefficient matrices is shown on the top side and right side of each matrix. Therefore, using the numerical assembly technique as done by the conventional finite element method (FEM) one may obtain a matrix equation for all the integration constants of the entire beam

$$[\overline{B}]\{\overline{C}\} = 0 \tag{47}$$

Non-trivial solution of Eq. (48) requires that its coefficient determinant is equal to zero, i.e.,

$$|\overline{B}| = 0 \tag{48}$$

Which is the frequency equation for the present problem.

In this paper, the incremental search method is used to find the natural frequencies of the vibrating system, ω_v $(v = 1, 2, \ldots)$. For each natural frequency ω_v, one may obtain the corresponding integration constants from Eq. (48). The substitution of the last integration constants into the displacement functions of the associated beam segments will determine the corresponding mode shape of the entire beam, $Y^{(v)}(\xi)$.

5. Numerical results and discussions

Before the free vibration analysis of a multi-step multi-span beam carrying multiple concentrated elements is performed, the reliability of the theory and the computer program developed for this paper are confirmed by comparing the present results with those obtained from the conventional finite element method (FEM). Besides, in FEM, the two-node beam elements are used and the entire beam is subdivided into 40 beam elements. Since each node has two degrees of freedom (DOF's), the total DOF for the entire unconstrained beam is 2(40 + 1) = 82. The dimensions of the three-step beam studied in this paper are (cf. Fig. 2): $d_1 = 0.05$ m, $d_2 = 0.075$ m, $d_3 = 0.10$ m and $d_4 = 0.15$ m; $L_1 = 0.2$ m, $L_2 = 0.3$ m, $L_3 = 0.25$ m and $L_4 = 0.25$ m. The total length of the stepped beam is $L = L_1 + L_2 + L_3 + L_4 = 1.0$ m; the locations for the step changes in cross-sections are $\xi_{r1} = 0.20$, $\xi_{r2} = 0.50$ and $\xi_{r3} = 0.75$; the mass density of beam is $\rho = 7.8 \times 10^3$ kg/m^3 and the Young's modulus is $E = 2.069 \times 10^{11}$ N/m^2. The reference mass is $\breve{m} = \overline{m}_1 L = 15.3153$ kg, the reference rotary is $\breve{J} = \overline{m}_1 L^3 = 15.3153$ kgm^2, the reference linear spring is $\breve{k}_T = EI_1/L = 6.34761 \times 10^4$ N/m and the reference rotational spring is $\breve{k}_R = EI_1/L = 6.34761 \times 10^4$ Nm/rad. Each beam segment is subdivided into ten beam elements; therefore, the lengths for each beam element in each beam segment are 0.02, 0.03, 0.025 and 0.025 m, respectively.

5.1 A single-span three-step beam carrying multiple concentrated elements excluding spring-mass systems

The first example is a pinned-pinned beam with three-step changes in circular cross-sections as

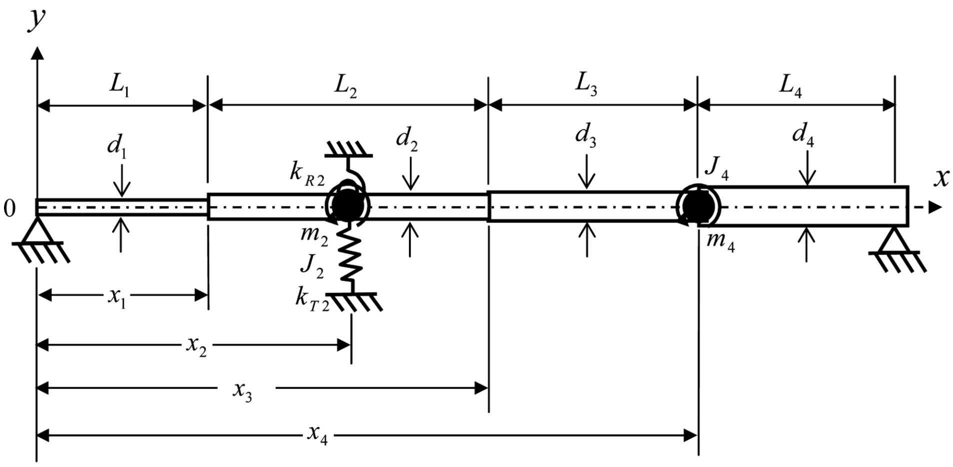

Fig. 2 Sketch for a pinned-pinned beam with three-step changes in cross-sections and carrying two point masses, two rotary inertias, one linear spring and one rotational spring

Table 1 The lowest five natural frequencies of the 3-step loaded beam shown in Fig. 2

Boundary conditions	Methods	Natural frequencies, ω_v (rad/sec)				
		ω_1	ω_2	ω_3	ω_4	ω_5
P-P	Present	645.8333	2144.4495	4415.9401	11513.0024	13503.7156
	FEM	645.8340	2144.4522	4415.9458	11513.0607	13503.7352
F-C	Present	749.5601	2287.0554	4306.2718	6333.2844	14849.3279
	FEM	749.5610	2287.0580	4306.2782	6333.2913	14849.4523
C-F	Present	100.0990	1173.3380	2725.6397	5212.7459	14968.9856
	FEM	100.0992	1173.3395	2725.6434	5212.7517	14969.1174

shown in Fig. 2 with diameter ratios $d_i^* = d_i/d_1 = 1.0$, 1.5, 2.0 and 3.0 ($i = 1-4$), and carrying two point masses, two rotary inertias, one linear spring and one rotational spring. The distributions of the concentrated elements are: there are a point mass m_2 with rotary inertia J_2, a linear spring k_{T2} and a rotational spring k_{R2} located at the intermediate point with $\xi_2 = x_2/L = 0.35$; there is a point mass m_4 with rotary inertia J_4 at $\xi_4 = 0.75$. The corresponding dimensionless parameters are: $m_2^* = m_2/\breve{m} = 1.0$, $J_2^* = J_2/\breve{J} = 0.04$, $k_{T2}^* = k_{T2}/\breve{k}_T = 1.0$, $k_{R2}^* = k_{R2}/\breve{k}_R = 1.0$, $m_4^* = 1.0$, $J_4^* = 0.02$. Three types of boundary conditions (P-P, F-C and C-F) are studied. Where P, C and F represent the abbreviations of pinned, clamped and free, respectively. The lowest five natural frequencies for the loaded beam with three boundary conditions are shown in Table 1. From the table one sees that the results of the present paper are in good agreement with those of FEM.

5.2 A single-span three-step beam carrying multiple concentrated elements including spring-mass systems

The second example is the same as the first one studied in the last subsection, but two additional intermediate spring-mass systems are carried as one may see from Fig. 3. The locations of the two spring-mass systems are at $\xi_4 = 0.6$ and $\xi_6 = 0.8$, respectively. The lowest five natural frequencies of the loaded beam are shown in Table 2, it is evident that the results of the present paper are also in good agreement with those of FEM.

From Table 2 one sees that the lowest two natural frequencies (ω_1 and ω_2) of either P-P or F-C loaded beam are close to the natural frequencies of the two spring-mass systems (with respect to the static beam) given by Eq. (24), $\hat{\omega}_4 = 192.6825$ rad/sec and $\hat{\omega}_6 = 248.7521$ rad/sec, respectively. Note that the subscripts 4 and 6 of $\hat{\omega}$ refer to the numberings of stations at which the spring-mass sysytems are attached. Besides, for the P-P and F-C loaded beams, the lowest 3-5 natural frequencies shown in Table 2 are close to the lowest 1-3 natural frequencies shown in Table 1. From the last phenomena one may conclude that, for the three-step P-P or F-C loaded beam as shown in Fig. 3, its lowest two natural frequencies are mainly due to the two spring-mass systems vibrating with respect to the static beam, while its lowest 3-5 ones are mainly due to the loaded beam. The situation for the C-F loaded beam is slightly different from that for the the P-P or F-C loaded beam: The lowest 2 and 3 natural frequencies of the C-F loaded beam shown in Table 2 are close to the natural frequencies of the two spring-mass systems with respect to the static beam (i.e., $\hat{\omega}_4 = 192.6825$ rad/sec and $\hat{\omega}_6 = 248.7521$ rad/sec), but the lowest 1, 4 and 5 are close to the lowest three ones of the C-F loaded beam shown in Table 1. This is because the lowest natural

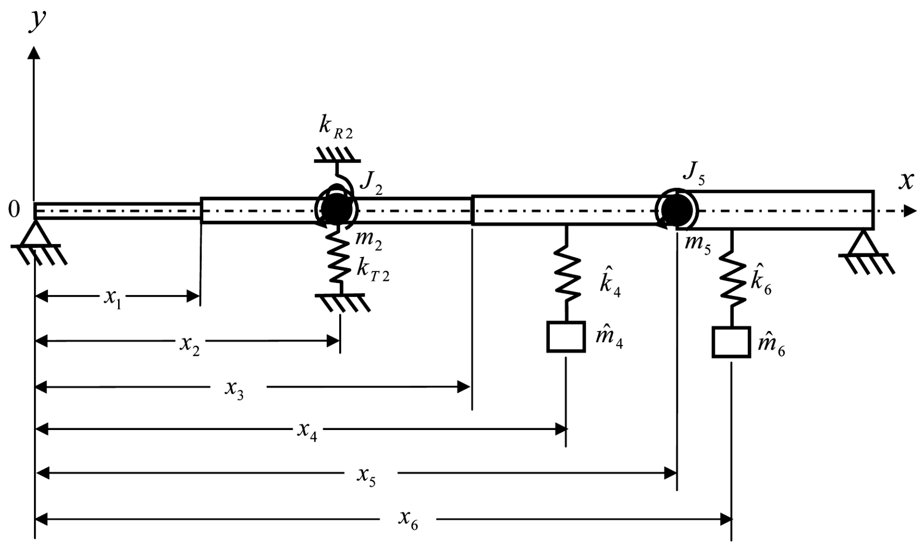

Fig. 3 Sketch for a pinned-pinned beam with three-step changes in cross-sections and carrying two point masses, two rotary inertias, one linear spring, one rotational spring and two spring-mass systems

Table 2 The lowest five natural frequencies of the 3-step loaded beam shown in Fig. 3

Boundry conditions	Methods	Natural frequencies, ω_v (rad/sec)				
		ω_1	ω_2	ω_3	ω_4	ω_5
P-P	Present	192.8043	248.3318	649.4005	2144.7423	4416.3347
	FEM	192.8049	248.3319	649.4016	2144.7447	4416.3401
F-C	Present	193.1215	249.2113	749.7701	2287.5297	4306.2761
	FEM	193.1221	249.2115	749.7707	2287.5325	4306.2826
C-F	Present	92.6318	205.5406	252.9763	1174.1703	2725.6832
	FEM	92.6320	205.5412	252.9766	1174.1723	2725.6868

frequency (ω_1) of the C-F loaded beam is lower than the natural frequencies of the two spring-mass systems with respect to the static beam (i.e., $\hat{\omega}_4$ = 192.6825 rad/sec and $\hat{\omega}_6$ = 248.7521 rad/sec).

5.3 A multi-span three-step beam with multiple concentrated elements

The third example is shown in Fig. 4, it is the same as the second one studied in the last subsection, except that there are three intermediate rigid (pinned) supports located at $\xi_i = x_i/L = 0.1$, 0.7 and 0.85, respectively, with i = 1, 6 and 9. It is similar to Tables 1 and 2 that the P-P beam, F-C beam and C-F beam are studied. For each kind of supporting conditions, three cases with total number of in-span supports N_s = 1, 2 and 3 are discussed. The results are shown in Table 3. From the table one sees that the lowest five natural frequencies of the loaded beam increase with increasing the total number of intermediate supports as expected and the present results are in good agreement with those obtained from the FEM.

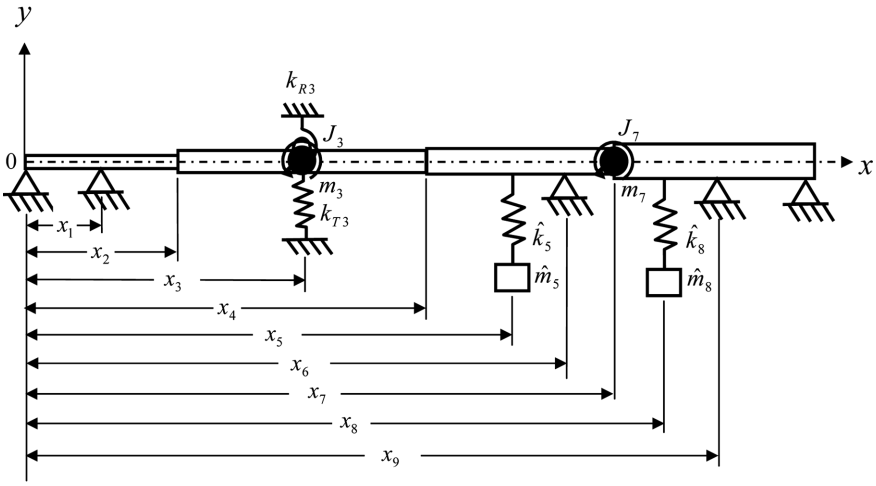

Fig. 4 Sketch for a pinned-pinned beam with three-step changes in cross-sections and carrying two point masses, two rotary inertias, one linear spring, one rotational spring, two spring-mass systems and having three intermediate pinned supports (i.e., $N_s = 3$)

Table 3 The lowest five natural frequencies of a three-step P-P, F-C or C-F beam carrying two lumped masses, two rotary inertias, one linear spring, one rotational spring, two spring-mass systems and having one to three intermediate pinned supports

Boundry conditions	Locations of In-span rigid supports, $\xi_s = x_s/L$	Methods	Natural frequencies, ω_v (rad/sec)				
			ω_1	ω_2	ω_3	ω_4	ω_5
P-P	0.10 *($N_s = 1$)	Present	192.9732	248.9206	1059.9582	3372.6617	4417.0620
		FEM	192.9737	248.9207	1059.9594	3372.6669	4417.0673
	0.10, 0.70 ($N_s = 2$)	Present	193.1335	249.3241	2986.5109	3484.6825	13381.4347
		FEM	193.1340	249.3244	2986.5151	3484.6876	13381.4527
	0.10, 0.70, 0.85 ($N_s = 3$)	Present	193.1358	249.3266	3108.1705	3507.1133	18318.3851
		FEM	193.1363	249.3269	3108.1744	3507.1189	18318.5502
F-C	0.10 ($N_s = 1$)	Present	193.1235	249.2590	1972.1805	3042.4729	6333.0737
		FEM	193.1239	249.2592	1972.1830	3042.4778	6333.0807
	0.10, 0.70 ($N_s = 2$)	Present	193.1346	249.3243	2561.1091	3371.7764	12291.7468
		FEM	193.1351	249.3246	2561.1126	3371.7814	12291.8055
	0.10, 0.70, 0.85 ($N_s = 3$)	Present	193.1358	249.3261	2607.8757	3421.0516	12296.6772
		FEM	193.1364	249.3263	2607.8790	3421.0568	12296.7361
C-F	0.10 ($N_s = 1$)	Present	114.1003	207.7561	253.2336	1404.2636	3454.0220
		FEM	114.1005	207.7565	253.2339	1404.2657	3454.0270
	0.10, 0.70 ($N_s = 2$)	Present	193.0501	249.2845	1215.6978	3406.3689	3671.6730
		FEM	193.0506	249.2848	1215.6993	3406.3741	3671.6779
	0.10, 0.70, 0.85 ($N_s = 3$)	Present	193.1358	249.3261	3112.3938	3523.5295	16998.2692
		FEM	193.1362	249.3264	3112.3985	3523.5352	16998.3572

*N_s = total number of in-span rigid (pinned-pinned) supports.

5.4 Mode Shapes of the three-step beams with multiple concentrated elements

Figs. 5(a)-(d) show the mode shapes corresponding to the lowest five eigenfrequencies of the P-P three-step beam (cf. Fig. 4). The diameter ratios for the three step changes in circular cross-sections are: $d_i^* = d_i/d_1$ = 1.0, 1.5, 2.0 and 3.0 and located at ξ_2 = 0.20, ξ_4 = 0.50 and ξ_7 = 0.75, respectively. In which, the 1st, 2nd, 3rd, 4th and 5th mode shapes are represented by the curves, −——, ············, ———, −−−, and —·—·—·, respectively. Note that Fig. 5(a) is for the "single-span" beam without attachment; Fig. 5(b) is for the "single-span" beam with two point masses, two rotary inertias, one linear spring, one rotational spring and two spring-mass systems; Fig. 5(c) is for the "two-span" beam with attachments the same as Fig. 5(b); Fig. 5(d) is for the "three-span" beam with attachments the same as Fig. 5(b).

For Fig. 5(b), the corresponding dimensionless parameters ($m_3^*, J_3^*, k_{T3}^*, k_{R3}^*, m_7^*, J_7^*, \hat{k}_5^*, \hat{m}_5^*, \hat{k}_8^*$ and $\hat{m}_8^*$) and the locations of step changes of cross-sections (ξ_2, ξ_4, ξ_7) are the same as subsection 4.2. The intermediate pinned support for the two-span beam is locatated at ξ_1 = 0.10, while the ones for

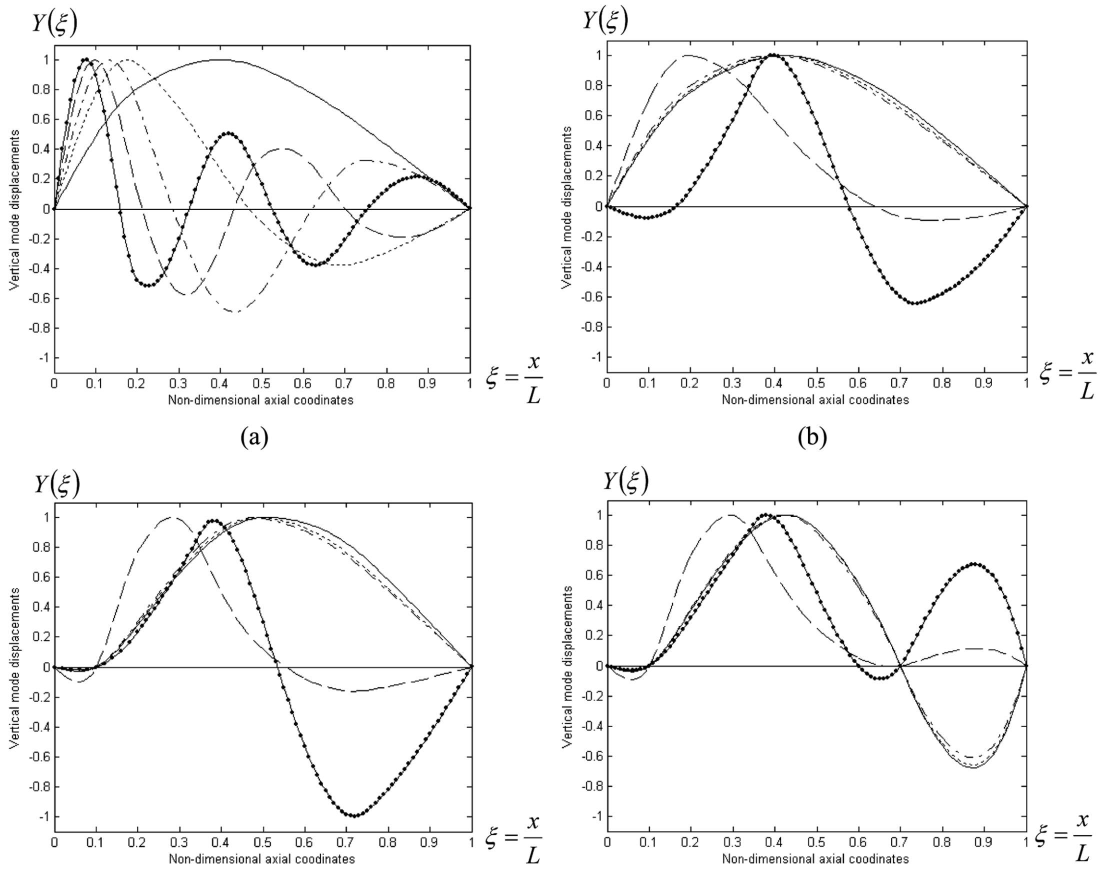

Fig. 5 The mode shapes corresponding to the lowest five eigenfrequencies of the P-P *three-step* beam (cf. Fig. 4): (a) *single span* without attachment; (b) *single span* with two lumped masses, two rotary inertias, one linear spring, one rotational spring and two spring-mass systems; (c) *two spans* with attachments the same as (b); (d) *three spans* with attachments the same as (b)

the three-span beam are locatated at ξ_1 = 0.10 and ξ_6 = 0.70, respectively.

From the mode shapes corresponding to the lowest five eigenfrequencies of the "single-span" beam carrying two point masses, two rotary inertias, one linear spring, one rotational spring and two

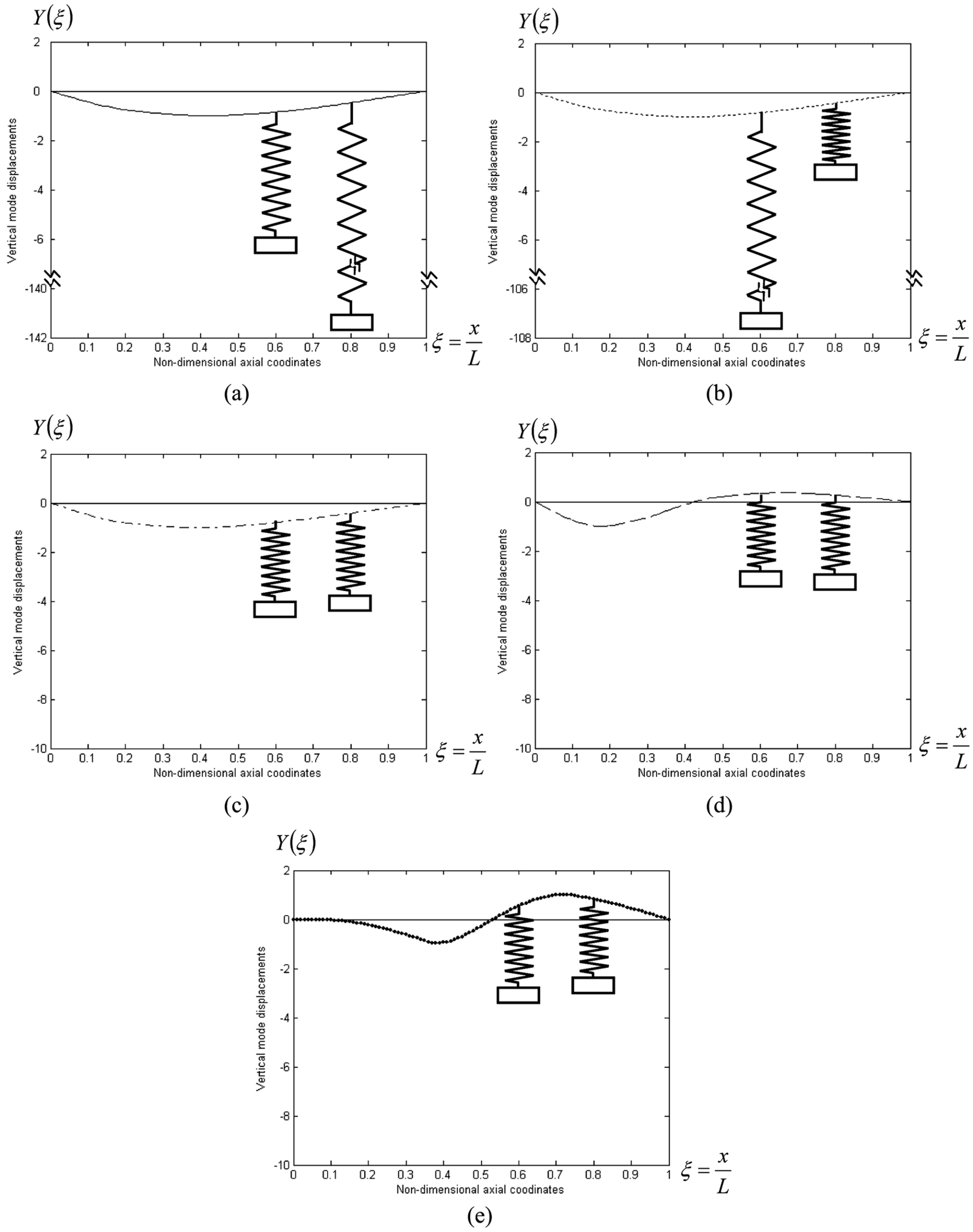

Fig. 6 The mode shapes corresponding to the lowest five eigenfrequencies of the three-step pinned-pinned beam carrying two lumped masses, two rotary inertias, one linear spring ,one rotational spring, two spring-mass systems (cf. Fig. 4): (a) first mode; (b) second mode; (c) third mode; (d) fourth mode; (e) fifth mode

spring-mass systems as shown in Fig. 5(b) one sees that the mode shapes corresponding to the lowest five eigenfrequencies of the loaded beam are very close to the 3rd one, this is because the 3rd natural frequency of the loaded beam (ω_3 = 649.4005 rad/sec) is very close to the 1st one of the bare beam (ω_{b1} = 645.8333 rad/sec) and the mode shapes corresponding to the lowest two eigenfrequencies of the loaded beam are close to the natural frequencies of the two spring-mass systems with respect to the static beam. In other words, the mode shapes corresponding to the lowest two eigenfrequencies of the loaded beam are major in the deformations of the two spring-mass systems and the 3rd mode shape is major in the deformation of the three-step beam itself as one may see from Figs. 6(a)-(c). Actually, from Figs. 6(d) and 6(e) one sees that the 4th and 5th mode shapes of the loaded beam are also major in the deformation of the three-step beam itself, therefore, the 4th and 5th mode shapes of the loaded beam shown in Fig. 5(b) are far from each other.

It is noted that the foregoing statements for the mode shapes corresponding to the lowest five eigenfrequencies of the single span beam shown Fig. 5(b) are also correct for those of the two-span beam shown in Fig. 5(c) and the three-span beam shown in Fig. 5(d). The mode shapes corresponding to the lowest five eigenfrequencies for the same three-step beam with F-C and C-F supporting conditions are shown in Figs. 7(a)-(d) and Figs. 8(a)-(d) for the single-span bare beam,

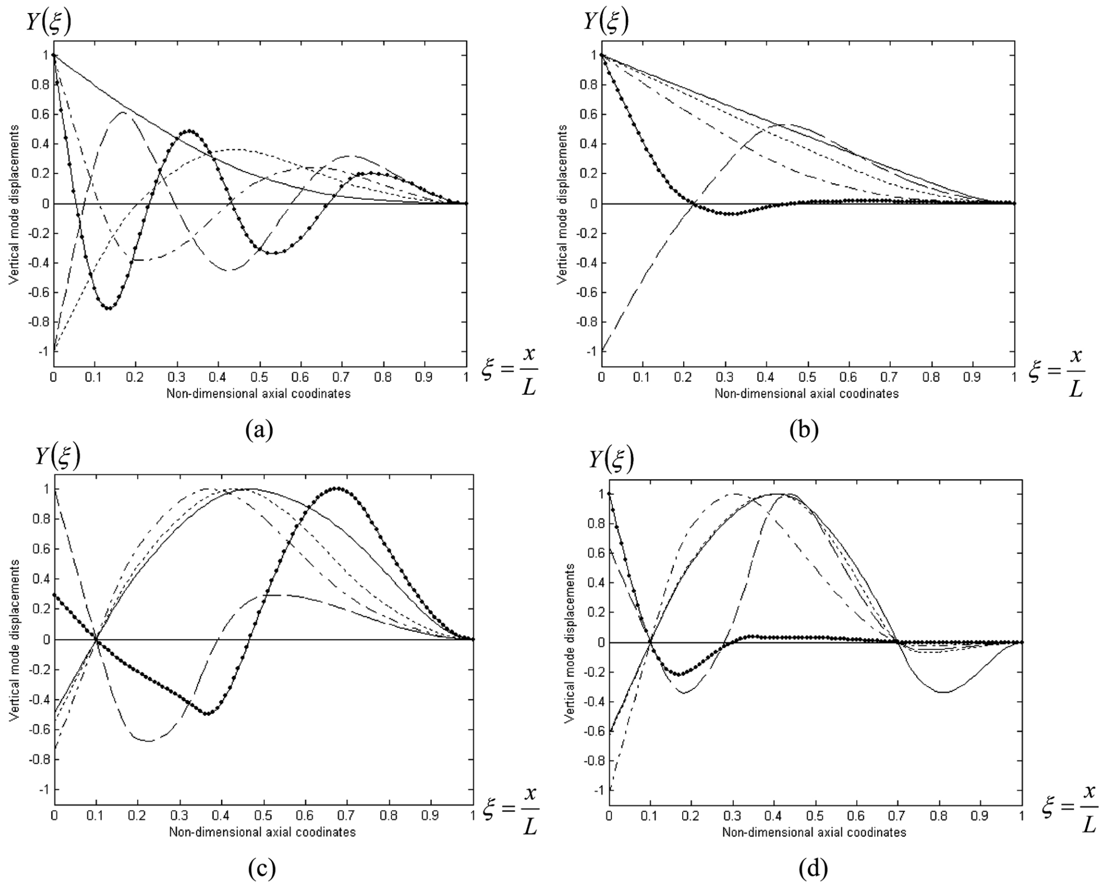

Fig. 7 The mode shapes corresponding to the lowest five eigenfrequencies of the F-C three-step loaded beams. Key as Fig. 5

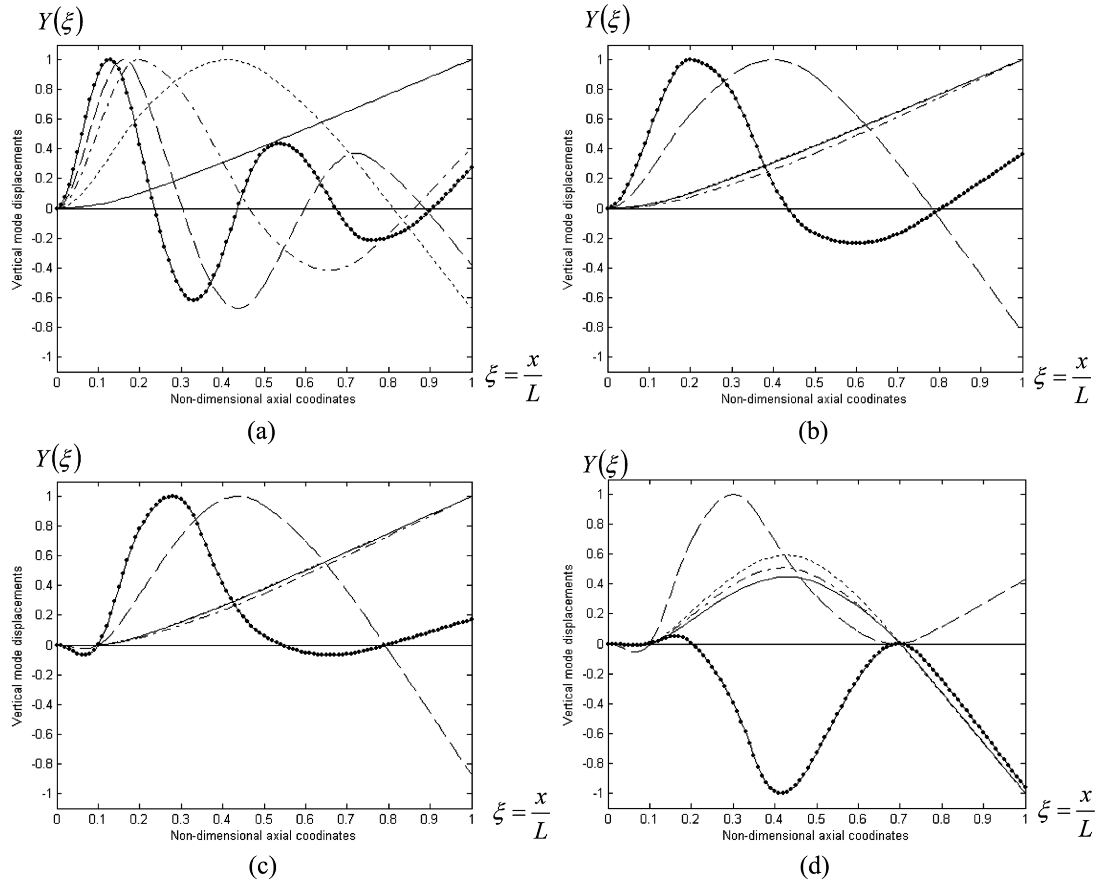

Fig. 8 The mode shapes corresponding to the lowest five eigenfrequencies of the C-F three-step beams. Key as Fig. 5

single-span loaded beam, two-span loaded beam and three-span loaded beam, respectively. Their keys are the same as those for Figs. 5(a)-(d).

6. Conclusions

From this study the following concluding remarks can be made:

1. Because the literature regarding the "exact" solutions for the natural frequencies and associated mode shapes of a multi-span beam with multi-step changes in cross sections and carrying multiple concentrated elements (such as point masses with rotary inertias, linear springs, rotational springs and/or spring-mass systems) are rare, and the classical analytical methods will suffer much difficulty for writing the high order (such as 38×38) explicit-form overall coefficient matrix [B] for calculating the value of the associated determinant |B|, the theory and the "exact" solutions for the examples presented in this paper will be useful for checking the accuracy of the numerical results obtained from various "approximate" methods.
2. For a beam carrying multiple spring-mass systems, if some of the natural frequencies (ω_i) of the

loaded beam is very close to some of the natural frequencies ($\hat{\omega}_j$) of the multiple spring-mass systems, then the corresponding mode shapes of the loaded beam are major in the deformations of some of the multiple spring-mass systems. On the other hand, the mode shapes of the loaded beam with corresponding natural frequencies (ω_r) far from the natural frequencies ($\hat{\omega}_s$) of the multiple spring-mass systems are major in the deformations of the loaded beam itself.

References

Balasubramanian, T.S. and Subramanian, G. (1985), "On the performance of a four- degree-of-freedom per node element for stepped beam analysis and higher frequency estimation", *J. Sound Vib.*, **99**(4), 563-567.

Balasubramanian, T.S., Subramanian, G. and Ramani, T.S. (1990), "Significance of very high order derivatives as nodal degrees of freedom in stepped beam vibration analysis", *J. Sound Vib.*, **137**(2), 353-356.

Chen, D.W. and Wu, J.S. (2002), "The exact solutions for the natural frequencies and mode shapes of non-uniform beams with multiple spring-mass systems", *J. Sound Vib.*, **255**(2), 299-322.

Chen, D.W. (2003), "The exact solutions for the natural frequencies and mode shapes of non-uniform beams carrying multiple various concentrated elements", *Struct. Eng. Mech.*, **16**(2), 153-176.

De Rosa, M.A. (1994), " Free vibrations of stepped beams with elastic ends", *J. Sound Vib.*, **173**(4), 557-563.

De Rosa, M.A., Belles, P.M. and Maurizi, M.J. (1995), "Free vibrations of stepped beams with intermediate elastic supports", *J. Sound Vib.*, **181**(5), 905-910.

Hamdan, M.N. and Abdel Latif, L. (1994), "On the numerical convergence of discretization methods for the free vibrations of beams with attached inertia elements", *J. Sound Vib.*, **169**(4), 527-545.

Jang, S.K. and Bert, C.W. (1989), "Free vibrations of stepped beams: exact and numerical solutions", *J. Sound Vib.*, **130**(2), 342-346.

Jang, S.K. and Bert, C.W. (1989), "Free vibrations of stepped beams: higher mode frequencies and effects of steps on frequency", *J. Sound Vib.*, **132**(1), 164-168.

Ju, F., Lee, H.P. and Lee, K.H. (1994), "On the free vibration of stepped beams", *Int. J. Solids Struct.*, **31**, 3125-3137.

Laura, P.A.A., Rossi, R.E., Pombo, J.L. and Pasqua, D. (1994), "Dynamic stiffening of straight beams of rectangular cross-section: a comparison of finite element predictions and experimental results", *J. Sound Vib.*, **150**(1), 174-178.

Lee, J. and Bergman, L.A. (1994), "Vibration of stepped beams and rectangular plates by an elemental dynamic flexibility method", *J. Sound Vib.*, **171**(5), 617-640.

Lin, H.Y. and Tsai, Y.C. (2005), "On the natural frequencies and mode shapes of a uniform multi-span beam carrying multiple point masses", *Struct. Eng. Mech.*, **21**(3), 351-367.

Lin, H.Y. and Tsai, Y.C. (2006), "On the natural frequencies and mode shapes of a multiple-step beam carrying a number of intermediate lumped masses and rotary inertias", *Struct. Eng. Mech.*, **22**(6), 701-717.

Lin, H.Y. and Tsai, Y.C. (2007), " Free vibration analysis of a uniform multi-span beam carrying multiple spring-mass systems", *J. Sound Vib.*, **302**(3), 442-456.

Maurizi, M.J. and Belles, P.M. (1994), "Natural frequencies of one-span beams with stepwise variable cross-section", *J. Sound Vib.*, **168**(1), 184-188.

Naguleswaran, S. (2002a), "Natural frequencies, sensitivity and mode shape details of an Euler-Bernoulli beam with one-step change in cross-section and with ends on classical supports", *J. Sound Vib.*, **252**(4), 751-767.

Naguleswaran, S. (200b), "Vibration of an Euler-Bernoulli beam on elastic end supports and with up to three step changes in cross-section", *Int. J. Mech. Sci.*, **44**, 2541-2555.

Subramanian, G. and Balasubramanian, T.S. (1985), "Beneficial effects of steps on the free vibration characteristics of beams", *J. Sound Vib.*, **118**(3), 555-560.

Wu, J.S. and Chou, H.M. (1998), "Free vibration analysis of a cantilever beam carrying any number of elastically mounted point masses with the analytical-and-numerical-combined method", *J. Sound Vib.*, **213**(2), 317-332.

Wu, J.S. and Chou, H.M. (1999), "A new approach for determining the natural frequencies and mode shapes of a uniform beam carrying any number of sprung masses", *J. Sound Vib.*, **220**(3), 451-468.

Appendix A

The coefficient matrix $[B_p]$ for Eq. (14) is given by

$$[B_p]=\begin{array}{c}\begin{matrix} 4p-3 & 4p-2 & 4p-1 & 4p & 4p+1 & 4p+2 & 4p+3 & 4p+4 \end{matrix} \\ \left[\begin{matrix} s\theta_{v,p} & c\theta_{v,p} & sh\theta_{v,p} & ch\theta_{v,p} & -s\theta_{v,p+1} & -c\theta_{v,p+1} & -sh\theta_{v,p+1} & -ch\theta_{v,p+1} \\ \Omega_{v,p}c\theta_{v,p} & -\Omega_{v,p}s\theta_{v,p} & \Omega_{v,p}ch\theta_{v,p} & \Omega_{v,p}sh\theta_{v,p} & -\Omega_{v,p+1}c\theta_{v,p+1} & \Omega_{v,p+1}s\theta_{v,p+1} & -\Omega_{v,p+1}ch\theta_{v,p+1} & -\Omega_{v,p+1}sh\theta_{v,p+1} \\ -\Omega^2_{v,p}s\theta_{v,p}+\alpha_p\Omega_{v,p}c\theta_{v,p} & -\Omega^2_{v,p}c\theta_{v,p}-\alpha_p\Omega_{v,p}s\theta_{v,p} & \Omega^2_{v,p}sh\theta_{v,p}+\alpha_p\Omega_{v,p}ch\theta_{v,p} & \Omega^2_{v,p}ch\theta_{v,p}+\alpha_p\Omega_{v,p}sh\theta_{v,p} & \varepsilon_p\Omega^2_{v,p+1}s\theta_{v,p+1} & \varepsilon_p\Omega^2_{v,p+1}c\theta_{v,p+1} & -\varepsilon_p\Omega^2_{v,p+1}sh\theta_{v,p+1} & -\varepsilon_p\Omega^2_{v,p+1}ch\theta_{v,p+1} \\ \sigma_p\Omega_{v,p}s\theta_{v,p}-\Omega^3_{v,p}c\theta_{v,p} & \sigma_p\Omega_{v,p}c\theta_{v,p}+\Omega^3_{v,p}s\theta_{v,p} & \sigma_p\Omega_{v,p}sh\theta_{v,p}+\Omega^3_{v,p}ch\theta_{v,p} & \sigma_p\Omega_{v,p}ch\theta_{v,p}+\Omega^3_{v,p}sh\theta_{v,p} & \varepsilon_p\Omega^3_{v,p+1}c\theta_{v,p+1} & -\varepsilon_p\Omega^3_{v,p+1}s\theta_{v,p+1} & -\varepsilon_p\Omega^3_{v,p+1}ch\theta_{v,p+1} & -\varepsilon_p\Omega^3_{v,p+1}sh\theta_{v,p+1} \end{matrix}\right]\begin{matrix} 4p-1 \\ 4p \\ 4p+1 \\ 4p+2 \end{matrix}\end{array} \tag{A1}$$

where

$$s\theta_{v,p} = \sin\Omega_{v,p}\xi_p, \quad c\theta_{v,p} = \cos\Omega_{v,p}\xi_p, \quad sh\theta_{v,p} = \sinh\Omega_{v,p}\xi_p, \quad ch\theta_{v,p} = \cosh\Omega_{v,p}\xi_p \tag{A2}$$

$$s\theta_{v,p+1} = \sin\Omega_{v,p+1}\xi_p, \quad c\theta_{v,p+1} = \cos\Omega_{v,p+1}\xi_p, \quad sh\theta_{v,p+1} = \sinh\Omega_{v,p+1}\xi_p, \quad ch\theta_{v,p+1} = \cosh\Omega_{v,p+1}\xi_p \tag{A3}$$

$$\alpha_p = -\left[J_p^*\Omega^4_{v,p}\left(\frac{\overline{m}_1}{\overline{m}_p}\right) - k^*_{Rp}\left(\frac{I_1}{I_p}\right)\right], \quad \sigma_p = \left[m_p^*\Omega^4_{v,p}\left(\frac{\overline{m}_1}{\overline{m}_p}\right) - k^*_{Tp}\left(\frac{I_1}{I_p}\right)\right], \quad \varepsilon_p = \frac{I_{p+1}}{I_p} \tag{A4}$$

Appendix B

The coefficient matrix $[B_u]$ for Eq. (25) is given by

$$[B_u]=\begin{array}{c}\begin{matrix} 4u-3 & 4u-2 & 4u-1 & 4u & 4u+1 & 4u+2 & 4u+3 & 4u+4 & 4u+5 \end{matrix} \\ \left[\begin{matrix} s\theta_{v,u} & c\theta_{v,u} & sh\theta_{v,u} & ch\theta_{v,u} & -s\theta_{v+1,u} & -c\theta_{v+1,u} & -sh\theta_{v+1,u} & -ch\theta_{v+1,u} & 0 \\ \Omega_{v,u}c\theta_{v,u} & -\Omega_{v,u}s\theta_{v,u} & \Omega_{v,u}ch\theta_{v,u} & \Omega_{v,u}sh\theta_{v,u} & -\Omega_{v+1,u}c\theta_{v+1,u} & \Omega_{v+1,u}s\theta_{v+1,u} & -\Omega_{v+1,u}ch\theta_{v+1,u} & -\Omega_{v+1,u}sh\theta_{v+1,u} & 0 \\ -\Omega^2_{v,u}s\theta_{v,u} & -\Omega^2_{v,u}c\theta_{v,u} & \Omega^2_{v,u}sh\theta_{v,u} & \Omega^2_{v,u}ch\theta_{v,u} & \varepsilon_u\Omega^2_{v+1,u}s\theta_{v+1,u} & \varepsilon_u\Omega^2_{v+1,u}c\theta_{v+1,u} & -\varepsilon_u\Omega^2_{v+1,u}sh\theta_{v+1,u} & -\varepsilon_u\Omega^2_{v+1,u}ch\theta_{v+1,u} & 0 \\ -\Omega^3_{v,u}c\theta_{v,u} & \Omega^3_{v,u}s\theta_{v,u} & \Omega^3_{v,u}ch\theta_{v,u} & \Omega^3_{v,u}sh\theta_{v,u} & \varepsilon_u\Omega^3_{v+1,u}c\theta_{v+1,u} & -\varepsilon_u\Omega^3_{v+1,u}s\theta_{v+1,u} & -\varepsilon_u\Omega^3_{v+1,u}ch\theta_{v+1,u} & -\varepsilon_u\Omega^3_{v+1,u}sh\theta_{v+1,u} & \hat{m}_u^*\Omega^4_{v,u} \\ s\theta_{v,u} & c\theta_{v,u} & sh\theta_{v,u} & ch\theta_{v,u} & 0 & 0 & 0 & 0 & \lambda_u^2-1 \end{matrix}\right]\begin{matrix} 4u-1 \\ 4u \\ 4u+1 \\ 4u+2 \\ 4u+3 \end{matrix}\end{array} \tag{B1}$$

Where

$$s\theta_{v,u} = \sin\Omega_{v,u}\xi_u, \quad c\theta_{v,u} = \cos\Omega_{v,u}\xi_u, \quad sh\theta_{v,u} = \sinh\Omega_{v,u}\xi_u, \quad ch\theta_{v,u} = \cosh\Omega_{v,u}\xi_u \tag{B2}$$

$$s\theta_{v,u+1} = \sin\Omega_{v,u+1}\xi_u, \quad c\theta_{v,u+1} = \cos\Omega_{v,u+1}\xi_u, \quad sh\theta_{v,u+1} = \sinh\Omega_{v,u+1}\xi_u, \quad ch\theta_{v,u+1} = \cosh\Omega_{v,u+1}\xi_u \tag{B3}$$

Appendix C

The coefficient matrix $[B_r]$ for Eq. (29) is given by

$$
[B_r]=\begin{array}{c}
\begin{array}{cccccccc}
4r-3 & 4r-2 & 4r-1 & 4r & 4r+1 & 4r+2 & 4r+3 & 4r+4
\end{array} \\
\left[\begin{array}{cccccccc}
\mathrm{s}\theta_{v,r} & \mathrm{c}\theta_{v,r} & \mathrm{sh}\theta_{v,r} & \mathrm{ch}\theta_{v,r} & 0 & 0 & 0 & 0 \\
0 & 0 & 0 & 0 & \mathrm{s}\theta_{v,r+1} & \mathrm{c}\theta_{v,r+1} & \mathrm{sh}\theta_{v,r+1} & \mathrm{ch}\theta_{v,r+1} \\
\Omega_{v,r}\mathrm{c}\theta_{v,r} & -\Omega_{v,r}\mathrm{s}\theta_{v,r} & \Omega_{v,r}\mathrm{ch}\theta_{v,r} & \Omega_{v,r}\mathrm{sh}\theta_{v,r} & -\Omega_{v,r+1}\mathrm{c}\theta_{v,r+1} & \Omega_{v,r+1}\mathrm{s}\theta_{v,r+1} & -\Omega_{v,r+1}\mathrm{ch}\theta_{v,r+1} & -\Omega_{v,r+1}\mathrm{sh}\theta_{v,r+1} \\
-\Omega_{v,r}^2\mathrm{s}\theta_{v,r} & -\Omega_{v,r}^2\mathrm{c}\theta_{v,r} & \Omega_{v,r}^2\mathrm{sh}\theta_{v,r} & \Omega_{v,r}^2\mathrm{ch}\theta_{v,r} & \varepsilon_r\Omega_{v,r+1}^2\mathrm{s}\theta_{v,r+1} & \varepsilon_r\Omega_{v,r+1}^2\mathrm{c}\theta_{v,r+1} & -\varepsilon_r\Omega_{v,r+1}^2\mathrm{sh}\theta_{v,r+1} & -\varepsilon_r\Omega_{v,r+1}^2\mathrm{ch}\theta_{v,r+1}
\end{array}\right]
\end{array}
\begin{array}{l}
\\ 4r-1 \\ 4r \\ 4r+1 \\ 4r+2
\end{array}
\tag{C1}
$$

where

$$\mathrm{s}\theta_{v,r}=\sin\Omega_{v,r}\xi_r,\quad \mathrm{c}\theta_{v,r}=\cos\Omega_{v,r}\xi_r,\quad \mathrm{sh}\theta_{v,r}=\sinh\Omega_{v,r}\xi_r,\quad \mathrm{ch}\theta_{v,r}=\cosh\Omega_{v,r}\xi_r \tag{C2}$$

$$\mathrm{s}\theta_{v,r+1}=\sin\Omega_{v,r+1}\xi_r,\quad \mathrm{c}\theta_{v,r+1}=\cos\Omega_{v,r+1}\xi_r,\quad \mathrm{sh}\theta_{v,r+1}=\sinh\Omega_{v,r+1}\xi_r,\quad \mathrm{ch}\theta_{v,r+1}=\cosh\Omega_{v,r+1}\xi_r \tag{C3}$$